

Terahertz-Band Direction Finding With Beam-Split and Mutual Coupling Calibration

Ahmet M. Elbir, *Senior Member, IEEE*, Kumar Vijay Mishra, *Senior Member, IEEE*,
and Symeon Chatzinotas, *Fellow, IEEE*

Abstract—Terahertz (THz) band is currently envisioned as the key building block to achieving the future sixth generation (6G) wireless systems. The ultra-wide bandwidth and very narrow beamwidth of THz systems offer the next order of magnitude in user densities and multi-functional behavior. However, wide bandwidth results in a frequency-dependent beampattern causing the beams generated at different subcarriers split and point to different directions. Furthermore, mutual coupling degrades the system’s performance. This paper studies the compensation of both beam-split and mutual coupling for direction-of-arrival (DoA) estimation by modeling the beam-split and mutual coupling as an array imperfection. We propose a subspace-based approach using multiple signal classification with CalibRated for beam-split and mutual coupling (CREAM-MUSIC) algorithm for this purpose. Via numerical simulations, we show the proposed CREAM-MUSIC approach accurately estimates the DoAs in the presence of beam-split and mutual coupling.

Index Terms—Array calibration, beam split, DoA estimation, mutual coupling, subspace-based harmonic retrieval, Terahertz.

I. INTRODUCTION

Terahertz (THz) band (0.1-10 THz) is widely viewed as a technology to enable significant performance enhancements in sixth-generation (6G) wireless networks [1]. An accuracy of milli-degree in direction-of-arrival (DoA) estimation is critical to guaranteeing the reliability of THz sensing as well as communications [2, 3]. However, significant challenges remain in realizing this goal at the THz band owing to high path losses, complex propagation/scattering phenomena, and the use of extremely large arrays [1, 4, 5].

In particular, the ultra-dense integration of the antennas in the THz array is accompanied by mutual coupling (MC) which leads to degradation in the direction finding accuracy [2, 6, 7]. The existing works on reducing MC in THz mostly involve array design with new metamaterials [8], graphene monolayers [9], THz metasurfaces [10] or frequency-selective graphene surfaces [7], while MC calibration at THz-band via signal processing remains relatively unexamined. Furthermore, THz arrays also suffer from *beam-split* arising from the subcarrier-independent (SI) analog beamformers (ABs) [11–13]. This causes the generated beams at different subcarriers split and point to different directions. At lower frequencies (e.g., up to millimeter-wave [14]), *beam-squint* is

used to describe the same phenomenon, and negative group-delay networks are used to compensate for it [15]. Whereas beam-squint causes slight deviations in the beam direction while they still cover the targets with their mainlobes, the generated beams are completely non-overlapping in *beam-split*. The latter is, therefore, a more severe form of the former (Fig. 1a). This angular deviation eventually impacts MC, which is direction-dependent because of the directional beampattern [16]. The existing techniques to mitigate beam-split are mostly hardware-based [11]. Specifically, additional hardware components such as time-delayer networks to realize subcarrier-dependent (SD) ABs, they are expensive because each phase shifter is connected to multiple delayer elements. Further, each such element consumes approximately 100 mW which is more than that of a single phase shifter (40 mW) at THz [3].

Although THz channel estimation [12] and hybrid analog/digital beamforming [11, 17] under beam-split have been explored in prior THz studies, these algorithms did not examine either DoA estimation or MC calibration. The hybrid architectures at mm-Wave [18, 19] and THz [2] so far employ orthogonal matching pursuit (OMP) [18], maximum likelihood (ML) [19] and *MU*ltiple *SI*gnal Classification (MUSIC) [2, 6] for DoA estimation but exclude beam-split and MC. The calibration of beam-split in THz systems is considered for different array geometries, e.g., uniform linear/rectangular array (ULA/URA) [12, 20, 21]. Specifically, the ULA provides a simple design whereas the URA-based THz systems allow a compact and efficient design with array/group of subarrays architecture [17]. While the calibration procedure is the similar, the use of URA introduces the calibration of beam-split in both azimuth and elevation.

In this work, contrary to previous works, we address the aforementioned shortcomings by considering beam-split as an array imperfection in a similar way as MC has been investigated in the well-studied array calibration theory [16, 22, 23]. Specifically, we model the beam-split errors as a diagonal matrix, which represents a linear transformation between the nominal and actual steering vectors corrupted by beam-split. Using this transformation and incorporating the signal-noise subspace orthogonality, we develop a *calibrated* for beam-split and MC MUSIC (CREAM-MUSIC) algorithm to obtain accurate DoA estimates. In particular, we introduce an alternating approach, wherein the DoAs, beam-split, and MC coefficients are iteratively estimated. For DoA, while the degree of beam-split is proportionally known *a priori*, it depends on the unknown target direction. For example,

This work was supported in part by the Horizon Project TERRAMETA.

A. M. Elbir is with the University of Luxembourg, Luxembourg; and Duzce University, Turkey (e-mail: ahmetmelbir@ieec.org).

K. V. Mishra is with the United States Army Research Laboratory, Adelphi, MD 20783 USA; and the University of Luxembourg, Luxembourg (e-mail: kvm@ieec.org).

S. Chatzinotas is with the University of Luxembourg, Luxembourg (e-mail: symeon.chatzinotas@uni.lu).

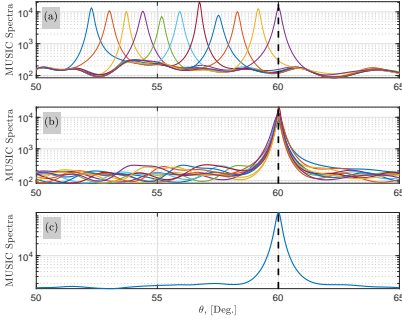


Fig. 1. The MUSIC spectra of (a) all subcarriers without beam-split compensation, (b) all subcarriers with beam-split compensation, (c) CREAM-MUSIC algorithm for the source location depicted with vertical line. $f_c = 300$ GHz, $B = 30$ GHz, $M = 11$, $\theta = 60^\circ$, $N = 128$ and $N_{\text{RF}} = 8$.

consider f_m and f_M to be the frequencies for, respectively, the m -th and last/highest subcarriers. When θ is the physical target direction, then the spatial direction corresponding to the m -th-subcarrier is shifted by $\frac{f_m}{f_M}\theta$. We then construct the CREAM-MUSIC spectra which accounts for this deviation and thereby *ipso facto* mitigates the effect of beam-split (Fig. 1b-c).

II. SYSTEM MODEL & PROBLEM FORMULATION

Consider a wideband THz ultra-massive multiple-input multiple-output uplink scenario, wherein the base-station (BS) employs hybrid analog/digital beamformers with N -element ULA and N_{RF} radio-frequency (RF) chains. In sensing applications, the equivalent signals would be from K targets. Without loss of generality, assume the targets are in the far-field of the BS with the physical DoAs θ_k for $k \in \{1, \dots, K\} = \mathcal{K}$, where $\theta_k = \sin \theta_k$ ($\tilde{\theta}_k \in [-\frac{\pi}{2}, \frac{\pi}{2}]$).

To begin with, we first consider the conventional MC- and beam-split- free scenario, wherein the $N \times 1$ steering vector corresponding to the k -th target is

$$\mathbf{a}(\theta_k) = [1, e^{j2\pi \frac{d}{\lambda^*} \theta_k}, \dots, e^{j2\pi(N-1) \frac{d}{\lambda^*} \theta_k}]^T, \quad (1)$$

where d stands for antenna spacing and $\lambda^* = \frac{\nu}{f_M}$ denotes the wavelength corresponding to the highest subcarrier frequency. Hence, d is selected as $d = \frac{\nu}{2 \max_m f_m} = \frac{\nu}{2f_M}$ in order to avoid spatial aliasing [24]. Here, ν is speed of light and $f_m = f_c + \frac{B}{M}(m-1 - \frac{M-1}{2})$ is the m -th subcarrier frequency ($m \in \{1, \dots, M\} = \mathcal{M}$) with f_c and B being the carrier frequency and total bandwidth, respectively.

In order to sense the targets, the BS employs the sensing signal $\mathbf{s}_m(t_i) \in \mathbb{C}^{N_{\text{RF}}}$ and the SI precoder $\mathbf{F} \in \mathbb{C}^{N \times N_{\text{RF}}}$. Then, the BS activates N_{RF} RF chains and applies $\mathbf{F} \in \mathbb{C}^{N \times N_{\text{RF}}}$ to the sensing signal $\mathbf{s}_m(t_i)$, and the $N \times 1$ transmit signal becomes $\mathbf{x}_m(t_i) = \mathbf{F} \mathbf{s}_m(t_i)$ where $i = 1, \dots, T$ and T is the number of data snapshots.

Beam-Split: During the search phase of the THz radar, the AB is designed with the structure of steering vectors corresponding to the search directions. For an arbitrary $\mathbf{a}(\theta_k)$ for direction θ_k . Then, the n -th element of $\mathbf{a}(\theta_k)$ is defined as $[\mathbf{a}(\theta_k)]_n = 1/\sqrt{N} \exp\{j(n-1)\frac{2\pi d}{\lambda_m} \theta_k\}$, i.e.,

$$[\mathbf{a}(\theta_k)]_n = 1/\sqrt{N} \exp\{j(n-1)\pi \eta_m \theta_k\}, \quad (2)$$

where $\eta_m = \frac{f_m}{f_M}$. We can see that the direction of AB designed for θ_k is split and points to the spatial direction $\bar{\theta}_{k,m} = \eta_m \theta_k$. It is also clear that when $f_m = f_M$, we have $\bar{\theta}_{k,m} = \theta_k$, which leads to the definition in (1).

Lemma 1. Let $\mathbf{a}(\bar{\theta}_m)$ and $\mathbf{a}(\theta)$ be the beam-split-corrupted and nominal steering vectors for an arbitrary direction θ and subcarrier $m \in \mathcal{M}$ as defined in (2) and (1), respectively. Then, $\mathbf{a}(\bar{\theta}_m)$ achieves the maximum array gain, i.e., $A_G(\theta, m) = \frac{|\mathbf{a}^H(\theta)\mathbf{a}(\bar{\theta}_m)|^2}{N^2}$, if $\bar{\theta}_m = \eta_m \theta$.

Proof. The array gain varies across the whole bandwidth as $A_G(\theta, m) = \frac{|\mathbf{a}^H(\theta)\mathbf{a}(\bar{\theta}_m)|^2}{N^2}$. By using (1) and (2), $A_G(\theta, m)$ is

$$\begin{aligned} A_G(\theta, m) &= \frac{1}{N^2} \left| \sum_{n_1=1}^N \sum_{n_2=1}^N e^{-j\pi((n_1-1)\bar{\theta}_m - (n_2-1)\frac{\lambda_M \theta}{\lambda_m})} \right|^2 \\ &= \left| \sum_{n=0}^{N-1} \frac{e^{-j2\pi n d (\frac{\bar{\theta}_m}{\lambda_M} - \frac{\theta}{\lambda_m})}}{N} \right|^2 = \left| \sum_{n=0}^{N_T-1} \frac{e^{-j2\pi n d (\frac{f_c \Phi_m - f_m \Phi}{c_0})}}{N} \right|^2 \\ &= \left| \frac{1 - e^{-j2\pi N d (\frac{f_M \bar{\theta}_m - f_m \theta}{\nu})}}{N(1 - e^{-j2\pi d (\frac{f_M \bar{\theta}_m - f_m \theta}{\nu})}} \right|^2 = \left| \frac{\sin(\pi N \mu_m)}{N \sin(\pi \gamma_m)} \right|^2 = |\xi(\mu_m)|^2, \end{aligned}$$

where $\mu_m = d \frac{(f_M \bar{\theta}_m - f_m \theta)}{\nu}$. The array gain implies that most of the power is focused only on a small portion of the beamspace due to the power-focusing capability of $\xi(\cdot)$, which substantially reduces across the subcarriers as $|f_m - f_M|$ increases. Furthermore, $|\xi(\mu_m)|^2$ gives peak when $\mu_m = 0$, i.e., $f_M \bar{\theta}_m - f_m \theta = 0$, which yields $\bar{\theta}_m = \eta_m \theta$. \square

Above lemma indicates that the split direction $\bar{\theta}_m$ should be taken into account to achieve accurate DoA estimation performance. Finally, we define the relationship between the nominal and beam-split-corrupted steering vectors as

$$\mathbf{a}(\bar{\theta}_{m,k}) = \mathbf{B}_{m,k} \mathbf{a}(\theta_k), \quad (3)$$

where $\mathbf{B}_{m,k} = \text{diag}\{b_{m,k,1}, \dots, b_{m,k,N}\}$ is an $N \times N$ diagonal matrix with $b_{m,k,n} = \exp\{j(n-1)\pi \Delta_{m,k}\}$, where $\Delta_{m,k}$ is defined as beam-split, i.e., $\Delta_{m,k} = \bar{\theta}_{m,k} - \theta_k$.

Mutual Coupling: Experimentally, the MC matrix is found from the inverse of the measurement transformation matrix $\mathbf{Z}_m \in \mathbb{C}^{N \times N}$, which maps the coupled voltages to the uncoupled voltages [25–27] as $\mathbf{Z}_m \mathbf{V}_m = \mathbf{U}_m$. Here, $\mathbf{V}_m = [\mathbf{v}_m^1, \dots, \mathbf{v}_m^\Omega] \in \mathbb{C}^{N \times \Omega}$ comprises the coupled measurements collected for $\Omega \geq N$ distinct directions when all the antennas are residing in the array whereas $\mathbf{U}_m = [\mathbf{u}_m^1, \dots, \mathbf{u}_m^\Omega] \in \mathbb{C}^{N \times \Omega}$ is obtained with N antenna elements, each of which is considered one-by-one separately while the remaining $N-1$ antennas are removed. Then, the direction-independent MC matrix is obtained as $\mathbf{C}_m = \mathbf{Z}_m^{-1}$. When the MC is DD, it should be computed for a certain angular sectors [16].

The MC matrix of a ULA¹ is represented by an L -banded Toeplitz matrix [22, 28, 29]. Define $\mathbf{C}_m(\theta_k) \in \mathbb{C}^{N \times N}$ as the SD and direction-dependent MC matrix with L MC coefficients, i.e.,

¹The proposed approach is easily applicable to different array geometries, e.g., UCA/URA. Specifically, the MC matrix has circular-symmetric and block-Toeplitz structure for UCA and URA, respectively [22].

$\mathbf{C}_m(\theta_k) = \text{Toeplitz}\{1, c_{m,k,1}, \dots, c_{m,k,L}, 0, \dots, 0\}$, where $\{c_{m,k,l}\}_{l=1}^L$ are the distinct MC coefficients. Denote the actual steering vector by $\tilde{\mathbf{a}}(\bar{\theta}_{m,k}) \in \mathbb{C}^N$. The steering vector corrupted by both beam-split and MC becomes

$$\tilde{\mathbf{a}}(\bar{\theta}_{m,k}) = \mathbf{C}_m(\theta_k)\mathbf{a}(\bar{\theta}_{m,k}) = \mathbf{C}_m(\theta_k)\mathbf{B}_{m,k}\mathbf{a}(\theta_k), \quad (4)$$

for which we define the MC-corrupted steering matrix in a compact form as $\mathbf{D}_m = [\tilde{\mathbf{a}}(\bar{\theta}_{m,1}), \dots, \tilde{\mathbf{a}}(\bar{\theta}_{m,K})] \in \mathbb{C}^{N \times K}$.

Our goal is to estimate the DoAs of the targets $\{\theta_k\}_{k=1}^K$ while accurately compensating for beam-split and MC.

III. PROPOSED METHOD

Define $\mathbf{X}_m = [\mathbf{x}_m(t_1), \dots, \mathbf{x}_m(t_T)] \in \mathbb{C}^{N \times T}$ as the radar probing signal transmitted by the BS for T data snapshots along the fast-time axis [30], where $\mathbb{E}\{\mathbf{X}_m\mathbf{X}_m^H\} = \frac{P_r T}{MN}\mathbf{I}_N$, for which $\mathbf{F}\mathbf{F}^H = 1/N$, and P_r is the radar transmit power. Limited number of RF chains yield $N_{\text{RF}} \times 1$ received baseband data vector. When $K \geq N_{\text{RF}}$, it results in poorer parameter estimation [24, 31]. To collect the full array data from N_{RF} RF chains, we follow a subarrayed approach. That is, the BS activates the antennas in a subarrayed manner to apply the $N \times N_{\text{RF}}$ analog beamforming matrix $\tilde{\mathbf{W}} = [\tilde{\mathbf{W}}_1^T, \dots, \tilde{\mathbf{W}}_J^T]^T$. Then, the BS collects the received target echoes for $J = \frac{N}{N_{\text{RF}}}$ time slots. The target DoAs remain invariant within a time slot but change across different time slots. This is reasonable for the THz system, wherein the symbol time is of the order of picoseconds [2, 30]. Then, for the j -th time slot, the BS applies the combiner matrix

$$\mathbf{W}_j = \begin{bmatrix} \mathbf{0}_{jN_{\text{RF}} \times N_{\text{RF}}} & \tilde{\mathbf{W}}_j \\ \mathbf{0}_{N-(j+1)N_{\text{RF}} \times N_{\text{RF}}} & \end{bmatrix} \in \mathbb{C}^{N \times N_{\text{RF}}}, \text{ where } \tilde{\mathbf{W}}_j \in \mathbb{C}^{N_{\text{RF}} \times N_{\text{RF}}}$$

represents the j -th block of $\tilde{\mathbf{W}}$ corresponding to the j -th subarray. Then, the $N_{\text{RF}} \times T$ echo signal from the K targets at the j -th time slot is

$$\mathbf{Y}_{m,j} = \sum_{k=1}^K \beta_k \mathbf{W}_j^H \tilde{\mathbf{a}}(\bar{\theta}_{m,k}) [\tilde{\mathbf{a}}(\bar{\theta}_{m,k})]^T \mathbf{X}_m + \tilde{\mathbf{N}}_{m,j}, \quad (5)$$

where $\beta_k \in \mathbb{C}$ denotes the reflection coefficient of the k -th target. $\tilde{\mathbf{N}}_{m,j} = \mathbf{W}_j^H \tilde{\mathbf{N}}_{m,j} \in \mathbb{C}^{N_{\text{RF}} \times T}$ is representing the noise term, where $\tilde{\mathbf{N}}_{m,j} = [\tilde{\mathbf{n}}_{m,j}(t_1), \dots, \tilde{\mathbf{n}}_{m,j}(t_T)] \in \mathbb{C}^{N \times T}$ with $\tilde{\mathbf{n}}_{m,j}(t_i) \sim \mathcal{CN}(\mathbf{0}, \sigma_n^2 \mathbf{I}_N)$. Denote the target steering matrix and reflection coefficients by $\mathbf{A}_{m,j} = \mathbf{W}_j^H \mathbf{D}_m \in \mathbb{C}^{N_{\text{RF}} \times K}$ and $\mathbf{\Pi} = \text{diag}\{\beta_1, \dots, \beta_K\} \in \mathbb{C}^{K \times K}$, then (5) becomes $\mathbf{Y}_{m,j} = \mathbf{A}_{m,j} \mathbf{\Pi} \mathbf{D}_m^T \mathbf{X}_m + \tilde{\mathbf{N}}_{m,j}$. Stacking all $\mathbf{Y}_{m,j}$ into a single $N \times T$ matrix leads to the overall observation matrix $\mathbf{Y}_m \in \mathbb{C}^{N \times T}$ as

$$\mathbf{Y}_m = [\mathbf{Y}_{m,1}^T, \dots, \mathbf{Y}_{m,J}^T]^T = \mathbf{A}_m \mathbf{\Pi} \mathbf{D}_m^T \mathbf{X}_m + \tilde{\mathbf{N}}_m, \quad (6)$$

where $\mathbf{A}_m = [\mathbf{A}_{m,1}^T, \dots, \mathbf{A}_{m,J}^T]^T = \mathbf{W}^H \mathbf{D}_m \in \mathbb{C}^{N \times K}$, $\mathbf{W} = [\mathbf{W}_1, \dots, \mathbf{W}_J] \in \mathbb{C}^{N \times N}$, and $\tilde{\mathbf{N}}_m = [\tilde{\mathbf{N}}_{m,1}^T, \dots, \tilde{\mathbf{N}}_{m,J}^T]^T$. We now introduce an alternating algorithm, wherein the beam-split-corrected DoA angles and the MC coefficients are estimated iteratively such that MC parameters are kept fixed while estimating the DoA angle or vice versa.

A. DoA and Beam-Split Estimation

In order to estimate the target directions, we invoke the wideband MUSIC algorithm [24, 31]. Define $\mathbf{R}_m \in \mathbb{C}^{N \times N}$ as the covariance matrix of \mathbf{Y}_m , i.e.,

$$\begin{aligned} \mathbf{R}_m &= \frac{1}{T} \mathbf{Y}_m \mathbf{Y}_m^H = \frac{1}{T} \mathbf{A}_m \left(\frac{P_r T}{MN} \tilde{\mathbf{\Pi}} \right) \mathbf{A}_m^H + \frac{1}{T} \tilde{\mathbf{N}}_m \tilde{\mathbf{N}}_m^H \\ &\cong \frac{P_r}{MN} \mathbf{A}_m \tilde{\mathbf{\Pi}} \mathbf{A}_m^H + \sigma_n^2 \mathbf{I}_N, \end{aligned} \quad (7)$$

where $\tilde{\mathbf{N}}_m \tilde{\mathbf{N}}_m^H \cong \sigma_n^2 T / N \mathbf{I}_N$ and $\tilde{\mathbf{\Pi}} \in \mathbb{C}^{K \times K}$ is defined as $\tilde{\mathbf{\Pi}} = \mathbf{\Pi} \mathbf{D}^T \mathbf{D}^* \mathbf{\Pi}^*$. Then, the eigendecomposition of \mathbf{R}_m yields $\mathbf{R}_m = \mathbf{U}_m \mathbf{\Theta}_m \mathbf{U}_m^H$, where $\mathbf{\Theta}_m \in \mathbb{C}^{N \times N}$ is a diagonal matrix composed of the eigenvalues of \mathbf{R}_m in a descending order, and $\mathbf{U}_m = [\mathbf{U}_m^S, \mathbf{U}_m^N] \in \mathbb{C}^{N \times N}$ corresponds to the eigenvector matrix; $\mathbf{U}_m^S \in \mathbb{C}^{N \times K}$ and $\mathbf{U}_m^N \in \mathbb{C}^{N \times N-K}$ are the signal and noise subspace eigenvector matrices, respectively. The columns of \mathbf{U}_m^S and \mathbf{A}_m span the same space that is orthogonal to the eigenvectors in \mathbf{U}_m^N as $\|\mathbf{U}_m^N^H (\mathbf{W}^H \tilde{\mathbf{a}}(\bar{\theta}_{m,k}))\|_2^2$, i.e., $\|\mathbf{U}_m^N^H (\mathbf{W}^H \mathbf{C}_m(\theta_k) \mathbf{B}_{m,k} \mathbf{a}(\theta_k))\|_2^2 = 0$, for $k \in \mathcal{K}$ and $m \in \mathcal{M}$ [31]. Thus, given the MC matrix $\mathbf{C}_m(\theta)$, the conventional MUSIC spectra is given by

$$P(\theta) = \sum_{m=1}^M P_m(\theta), \quad (8)$$

where $P_m(\theta)$ is the spectrum corresponding to the m -th subcarrier as $P_m(\theta) = \frac{1}{f(m,k)}$, where $f(m,k) = \mathbf{a}^H(\theta) \mathbf{C}_m^H(\theta) \mathbf{W} \mathbf{U}_m^N \mathbf{U}_m^N^H \mathbf{W}^H \mathbf{C}_m(\theta) \mathbf{a}(\theta)$. The MUSIC spectra in (8) yields MK peaks, which are deviated due to beam-split (see Fig. 1a) while correct MUSIC spectra should include K peaks which are aligned for $m \in \mathcal{M}$. In other words, beam-split-corrected steering vectors should be used to accurately compute the MUSIC spectra. The CREAM-MUSIC accounts for this deviation by employing *beam-split-aware* steering vectors $\mathbf{e}_m(\theta) = \mathbf{W}^H \mathbf{C}_m(\theta) \mathbf{a}(\bar{\theta}_m) \in \mathbb{C}^N$. Then, the CREAM-MUSIC spectra is $\tilde{P}(\theta) = \sum_{m=1}^M \tilde{P}_m(\theta)$, where

$$\tilde{P}_m(\theta) = \frac{1}{\mathbf{e}_m^H(\theta) \mathbf{U}_m^N \mathbf{U}_m^N^H \mathbf{e}_m(\theta)}, \quad (9)$$

for which, the K highest peaks of (9) correspond to the estimated target DoAs $\{\theta_k\}_{k=1}^K$, and the beam-split is computed as $\hat{\Delta}_{m,k} = (\eta_m - 1)\theta_k$, for $m \in \mathcal{M}$, $k \in \mathcal{K}$. Note that combining the spectra of M subcarriers results in only a single peak-search in place of separately estimating the DoAs for each subcarrier.

B. Mutual Coupling Estimation

Define $\mathbf{c}_{m,k} = [c_{m,k,1}, \dots, c_{m,k,L}]^T$ as the $L \times 1$ vector MC coefficients. Then, we construct the following useful matrix-vector transformation between $\mathbf{c}_{m,k}$ and $\mathbf{C}_m(\theta_k)$, i.e., $\mathbf{C}_m(\theta_k) = \mathbf{T}_{m,k} \mathbf{c}_{m,k}$, where $\mathbf{T}_{m,k} = [\mathbf{S}_{m,1} \mathbf{a}(\bar{\theta}_{m,k}), \dots, \mathbf{S}_{m,L} \mathbf{a}(\bar{\theta}_{m,k})] \in \mathbb{C}^{N \times L}$, for which $\mathbf{S}_{m,l}$ is an $N \times N$ matrix, and it is defined for any array geometry as $\mathbf{S}_{m,l} = \begin{cases} 1, & \text{if } [\mathbf{C}_m(\theta_k)]_{i,j} = c_{m,k,l} \\ 0, & \text{otherwise} \end{cases}$ [16].

Given the DoAs $\{\theta_k\}_{k=1}^K$, we solve the following optimization problem to estimate $\mathbf{c}_{m,k}$, i.e.,

minimize $\mathbf{c}_{m,k}$ $\sum_{m=1}^M f(m,k)$, s. t.: $\mathbf{c}_{m,k,1} = 1$, which is equivalent to minimize $\mathbf{c}_{m,k}$ $\sum_{m=1}^M \mathbf{c}_{m,k}^H \Sigma_{m,k} \mathbf{c}_{m,k}$, s. t.: $\mathbf{v}^T \mathbf{c}_{m,k} = 1$, where $\mathbf{v} = [1, 0, \dots, 0]^T \in \mathbb{C}^{L \times 1}$ and $\Sigma_{m,k} \in \mathbb{C}^{L \times L}$ is $\Sigma_{m,k} = \mathbf{T}_{m,k}^H \mathbf{W} \mathbf{U}_m^N \mathbf{U}_m^N \mathbf{H} \mathbf{W}^H \mathbf{T}_{m,k}$. Then, the closed-form solution for $\mathbf{c}_{m,k}$ is

$$\hat{\mathbf{c}}_{m,k} = \Sigma_{m,k}^{-1} \mathbf{v} \left(\mathbf{v}^T \Sigma_{m,k}^{-1} \mathbf{v} \right)^{-1}. \quad (10)$$

In Algorithm 1, we present the proposed alternating approach to effectively estimate the DoAs, beam-split, and MC coefficients. Specifically, we first partition the angular search space into S sectors as $\Phi = \cup_{s=1}^S \Psi_s$, where $\Phi = [-\frac{\pi}{2}, \frac{\pi}{2}]$ for a ULA, and Ψ_s denotes the angular sector, for which the direction-dependent MC matrix $\mathbf{C}_m(\Psi_s)$ is kept fixed [16]. Then, the estimates of the DoAs and MC coefficients are alternately computed until the algorithm converges for a predefined error threshold parameter ϵ . While the alternating algorithm does not guarantee optimality, its convergence has been shown in prior works [22, 29]. Nevertheless, the proposed approach almost achieves the CRB (see Fig. 2).

The implementation of CREAM-MUSIC is similar to the other alternating algorithms for DoA and MC estimation and beam-split compensation stage does not impose an additional constraint on the problem. The computational complexity of the proposed approach is similar to the existing techniques [22, 28, 29] except that wideband processing is involved. Therefore, the complexity order is $\mathcal{O}(M[N^3 + KL^3])$ because of eigendecomposition for DoA estimation ($\mathcal{O}(MN^3)$) and computation of the direction-dependent MC coefficients ($\mathcal{O}(MKL^3)$) for M subcarriers.

IV. NUMERICAL EXPERIMENTS

We evaluate the performance of our CREAM-MUSIC approach in comparison with the MUSIC algorithm with no calibration, only beam-split compensation (BSC), and only MC calibration (MCC), as well as the Cramér-Rao bound (CRB) [12], in terms of root mean-squared-error (RMSE), i.e., $\text{RMSE}_\theta = \left(\frac{1}{J_T K} \sum_{i=1}^{J_T} \sum_{k \in \mathcal{K}} \|\hat{\theta}_{i,k} - \theta_{i,k}\|_2^2 \right)^{1/2}$, where $\hat{\theta}_{i,k}$ stands for the estimated DoA for the i -th experiment of $J_T = 100$ Monte Carlo trials. The simulation parameters are $f_c = 300$ GHz, $B = 30$ GHz, $M = 64$, $N = 128$, $N_{\text{RF}} = 8$, $T = 100$, $K = 2$ and $L = 5$ [2, 16, 17]. Our CREAM-MUSIC method in Algorithm 1 is run approximately for $\ell = 50$ iterations with $\epsilon = 10^{-4}$. The DoAs are selected uniform randomly as $\tilde{\theta}_k \sim \text{unif}[-\frac{\pi}{2}, \frac{\pi}{2}]$. The AB matrix is modeled as $[\mathbf{W}]_{i,j} = \frac{1}{\sqrt{N}} e^{j\psi}$, where $\psi \sim \text{unif}[-1, 1]$ for $i = 1, \dots, N$ and $j = 1, \dots, N_{\text{RF}}$. The direction-dependent MC coefficient vectors are selected as $\mathbf{c}_{m,1} = [0.85e^{j\varphi_{m,1,1}}, 0.8e^{j\varphi_{m,1,2}}, 0.4e^{j\varphi_{m,1,3}}, 0.2e^{j\varphi_{m,1,4}}]^T$ and $\mathbf{c}_{m,2} = [0.9e^{j\varphi_{m,2,1}}, 0.75e^{j\varphi_{m,2,2}}, 0.45e^{j\varphi_{m,2,3}}, 0.25e^{j\varphi_{m,2,4}}]^T$, where $\varphi_{k,l} \sim \text{unif}[-\pi, \pi]$ for $m \in \mathcal{M}$ and $l = 1, \dots, L$.

In Fig. 2, we present the DoA estimation RMSE with respect to signal-to-noise-ratio (SNR), which is defined as $\text{SNR} = 10 \log_{10}(\frac{\rho}{\sigma_n^2})$, where $\rho = \frac{P_s}{MN^2} = 1$. As it is seen, both MUSIC and MCC-MUSIC have poor performance because they do not take into account the effect of beam-split. In contrast, BSC-MUSIC exhibits lower RMSE than

Algorithm 1 CREAM-MUSIC

Input: $\mathbf{Y}_m, \mathbf{W}, K, S, \Phi, \epsilon, \eta_m$.
1: **Initialize:** $\ell = 1, \mathbf{C}_m^\ell(\Psi_s) = \mathbf{I}_N, m \in \mathcal{M}, k \in \mathcal{K}$.
2: **while** not terminated **do**
3: **for** $m \in \mathcal{M}$
4: Compute \mathbf{R}_m and \mathbf{U}_m^N from (7).
5: **for** $s = 1, \dots, S$ **do**
6: Compute $\tilde{P}_m^\ell(\Psi_s)$ from (9) using $\mathbf{C}_m^\ell(\Psi_s)$.
7: **end**
8: Construct $\tilde{P}_m^\ell(\Phi) = \cup_{s=1}^S \tilde{P}_m^\ell(\Psi_s)$.
9: **end**
10: $\tilde{P}^\ell(\Phi) \leftarrow \sum_{m=1}^M \tilde{P}_m^\ell(\Phi)$.
11: Find $\{\hat{\theta}_k^\ell\}_{k=1}^K$ from the K highest peaks of $\tilde{P}^\ell(\Phi)$.
12: **for** $k \in \mathcal{K}, m \in \mathcal{M}$
13: $\hat{\Delta}_{m,k}^\ell \leftarrow (\eta_m - 1)\hat{\theta}_k^\ell$.
14: **end**
15: Solve (10) for $\hat{\mathbf{C}}_m^\ell(\theta_k)$ by using $\mathbf{a}(\hat{\theta}_k^\ell)$, $m \in \mathcal{M}, k \in \mathcal{K}$.
16: **if** $\sum_{k \in \mathcal{K}} |\hat{\theta}_k^\ell - \hat{\theta}_k^{\ell-1}| \leq \epsilon$ **then** terminate **end**
17: $i \leftarrow i + 1$
18: **end**
Return: $\hat{\theta}_k, \hat{\Delta}_{m,k}$ and $\hat{\mathbf{C}}_m(\theta_k)$ for $m \in \mathcal{M}, k \in \mathcal{K}$.

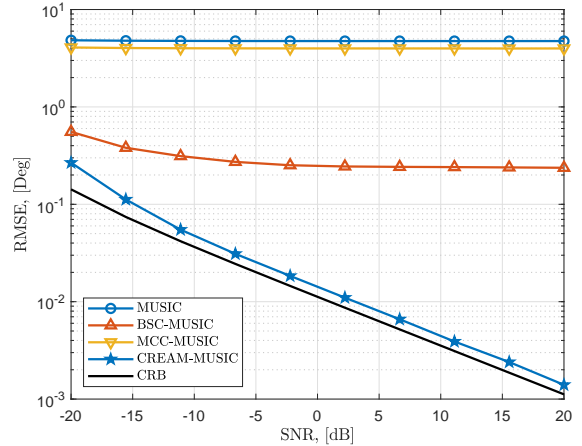


Fig. 2. DoA estimation RMSE vs. SNR.

that of MCC-MUSIC. Specifically, DoA estimation error due to beam-split and MC is approximately 4° and 0.25° , respectively. The significance of the DoA error due to beam-split is directly related to η_m (see Fig.1a), which causes deviations in the steering vector model (see (2)). This clearly shows the importance of beam-split compensation. In high SNR, the performance of BSC-MUSIC maxes out due to lose of precision, while the proposed CREAM-MUSIC approach attains the CRB very closely and outperforms the remaining methods yielding poor precision.

V. SUMMARY

We examined the THz DoA estimation problem in the presence of beam-split and MC. While the latter has a marginal impact ($\sim 0.25^\circ$) on DoA estimation, the former causes significant errors in the array gain and be severe ($\sim 4^\circ$). We showed that the proposed CREAM-MUSIC approach can effectively compensate both DoA errors due to beam-split and MC. Furthermore, the proposed method does not require additional hardware components, e.g., time-delayer networks for beam-split calibration.

REFERENCES

- [1] I. F. Akyildiz, C. Han, Z. Hu, S. Nie, and J. M. Jornet, "Terahertz Band Communication: An Old Problem Revisited and Research Directions for the Next Decade," *IEEE Trans. Commun.*, vol. 70, no. 6, pp. 4250–4285, May 2022.
- [2] Y. Chen, L. Yan, C. Han, and M. Tao, "Millidegree-Level Direction-of-Arrival Estimation and Tracking for Terahertz Ultra-Massive MIMO Systems," *IEEE Trans. Wireless Commun.*, vol. 21, no. 2, pp. 869–883, Aug. 2021.
- [3] A. M. Elbir, K. V. Mishra, S. Chatzinotas, and M. Bennis, "Terahertz-Band Integrated Sensing and Communications: Challenges and Opportunities," *arXiv*, Aug. 2022.
- [4] H. Sardeddeen, M.-S. Alouini, and T. Y. Al-Naffouri, "An overview of signal processing techniques for Terahertz communications," *Proceedings of the IEEE*, vol. 109, no. 10, pp. 1628–1665, 2021.
- [5] S. Venkatesh, X. Lu, H. Saeidi, and K. Sengupta, "A Programmable Terahertz Metasurface With Circuit-Coupled Meta-Elements in Silicon Chips: Creating Low-Cost, Large-Scale, Reconfigurable Terahertz Metasurfaces," *IEEE Antennas Propag. Mag.*, vol. 64, no. 4, pp. 110–122, Jun. 2022.
- [6] H. Nayir, G. K. Kurt, and A. Görçin, "Angle of Arrival Estimation for Terahertz-enabled Space Information Networks," in *2022 IEEE Future Networks World Forum (FNWF)*. IEEE, Oct. 2022, pp. 153–157.
- [7] B. Zhang, J. M. Jornet, I. F. Akyildiz, and Z. P. Wu, "Mutual Coupling Reduction for Ultra-Dense Multi-Band Plasmonic Nano-Antenna Arrays Using Graphene-Based Frequency Selective Surface," *IEEE Access*, vol. 7, pp. 33 214–33 225, Mar. 2019.
- [8] A. Jafarholi, A. Jafarholi, and J. H. Choi, "Mutual Coupling Reduction in an Array of Patch Antennas Using CLL Metamaterial Superstrate for MIMO Applications," *IEEE Trans. Antennas Propag.*, vol. 67, no. 1, pp. 179–189, Oct. 2018.
- [9] G. Moreno, H. M. Bernety, and A. B. Yakovlev, "Reduction of Mutual Coupling Between Strip Dipole Antennas at Terahertz Frequencies With an Elliptically Shaped Graphene Monolayer," *IEEE Antennas Wirel. Propag. Lett.*, vol. 15, pp. 1533–1536, Dec. 2015.
- [10] M. Alibakhshikenari, C. H. See, B. S. Virdee, and R. A. Abd-Alhameed, "Meta-Surface Wall Suppression of Mutual Coupling between Microstrip Patch Antenna Arrays for THz-Band Applications," 2018, [Online; accessed 8. Apr. 2023]. [Online]. Available: <https://bradscholars.brad.ac.uk/handle/10454/15908>
- [11] J. Tan and L. Dai, "Wideband Beam Tracking in THz Massive MIMO Systems," *IEEE J. Sel. Areas Commun.*, vol. 39, no. 6, pp. 1693–1710, Apr 2021.
- [12] A. M. Elbir, W. Shi, A. K. Papazafeiropoulos, P. Kourtessis, and S. Chatzinotas, "Terahertz-Band Channel and Beam Split Estimation via Array Perturbation Model," *IEEE Open J. Commun. Soc.*, p. 1, Mar. 2023.
- [13] A. M. Elbir, K. V. Mishra, S. A. Vorobyov, and R. W. Heath, "Twenty-Five Years of Advances in Beamforming: From convex and nonconvex optimization to learning techniques," *IEEE Signal Process. Mag.*, vol. 40, no. 4, pp. 118–131, Jun. 2023.
- [14] B. Wang, F. Gao, S. Jin, H. Lin, and G. Y. Li, "Spatial- and Frequency-Wideband Effects in Millimeter-Wave Massive MIMO Systems," *IEEE Trans. Signal Process.*, vol. 66, no. 13, pp. 3393–3406, May 2018.
- [15] H. Mirzaei and G. V. Eleftheriades, "Arbitrary-Angle Squint-Free Beamforming in Series-Fed Antenna Arrays Using Non-Foster Elements Synthesized by Negative-Group-Delay Networks," *IEEE Trans. Antennas Propag.*, vol. 63, no. 5, pp. 1997–2010, Feb. 2015.
- [16] A. M. Elbir, "Direction Finding in the Presence of Direction-Dependent Mutual Coupling," *IEEE Antennas Wirel. Propag. Lett.*, vol. 16, pp. 1541–1544, Jan. 2017.
- [17] A. M. Elbir, K. V. Mishra, and S. Chatzinotas, "Terahertz-Band Joint Ultra-Massive MIMO Radar-Communications: Model-Based and Model-Free Hybrid Beamforming," *IEEE J. Sel. Top. Signal Process.*, vol. 15, no. 6, pp. 1468–1483, Oct. 2021.
- [18] D. Fan, Y. Deng, F. Gao, Y. Liu, G. Wang, Z. Zhong, and A. Nallanathan, "Training Based DOA Estimation in Hybrid mmWave Massive MIMO Systems," in *GLOBECOM 2017 - 2017 IEEE Global Communications Conference*. IEEE, Dec. 2017, pp. 1–6.
- [19] R. Zhang, B. Shim, and W. Wu, "Direction-of-Arrival Estimation for Large Antenna Arrays With Hybrid Analog and Digital Architectures," *IEEE Trans. Signal Process.*, vol. 70, pp. 72–88, Oct. 2021.
- [20] A. M. Elbir and S. Chatzinotas, "BSA-OMP: Beam-Split-Aware Orthogonal Matching Pursuit for THz Channel Estimation," *IEEE Wireless Commun. Lett.*, vol. 12, no. 4, pp. 738–742, Feb. 2023.
- [21] A. M. Elbir, "A Unified Approach for Beam-Split Mitigation in Terahertz Wideband Hybrid Beamforming," *IEEE Trans. Veh. Technol.*, pp. 1–6, Apr. 2023.
- [22] B. Friedlander and A. J. Weiss, "Direction finding in the presence of mutual coupling," *IEEE Trans. Antennas Propag.*, vol. 39, no. 3, pp. 273–284, Mar. 1991.
- [23] M. Viberg, M. Lanne, and A. Lundgren, "Calibration in Array Processing," in *Classical and Modern Direction-of-Arrival Estimation*. Cambridge, MA, USA: Academic Press, Jan. 2009, pp. 93–124.
- [24] B. Friedlander and A. J. Weiss, "Direction finding for wide-band signals using an interpolated array," *IEEE Trans. Signal Process.*, vol. 41, no. 4, pp. 1618–1634, 1993.
- [25] I. Gupta and A. Ksienski, "Effect of mutual coupling on the performance of adaptive arrays," *IEEE Trans. Antennas Propag.*, vol. 31, no. 5, pp. 785–791, Sep. 1983.
- [26] H. T. Hui, "A practical approach to compensate for the mutual coupling effect in an adaptive dipole array," vol. 52, no. 5, pp. 1262–1269, May 2004.
- [27] A. M. Elbir and T. E. Tuncer, "Calibration of antenna arrays for aeronautical vehicles on ground," *Aerosp. Sci. Technol.*, vol. 30, no. 1, pp. 18–25, Oct. 2013.
- [28] A. M. Elbir, "Calibration of directional mutual coupling for antenna arrays," *Digital Signal Process.*, vol. 69, pp. 117–126, Oct. 2017.
- [29] B. Liao, Z.-G. Zhang, and S.-C. Chan, "DOA Estimation and Tracking of ULAs with Mutual Coupling," *IEEE Trans. Aerosp. Electron. Syst.*, vol. 48, no. 1, pp. 891–905, Jan. 2012.
- [30] X. Yu, G. Cui, J. Yang, L. Kong, and J. Li, "Wideband MIMO radar waveform design," *IEEE Trans. Signal Process.*, vol. 67, no. 13, pp. 3487–3501, 2019.
- [31] R. Schmidt, "Multiple emitter location and signal parameter estimation," *IEEE Trans. Antennas Propag.*, vol. 34, no. 3, pp. 276–280, Mar. 1986.